

Non-Radiative Recombination Center in AlGaInP Quarternary Alloys

K. Sugiura, K. Domen, C. Anayama, M. Kondo, M. Sugawara,
T. Tanahashi and K. Nakajima

Fujitsu Laboratories Ltd.,
10-1 Morinosato-Wakamiya, Atsugi 243-01, Japan

We investigated deep energy levels in undoped-AlGaInP grown by metal organic vapor phase epitaxy using capacitance transient spectroscopy. We found three deep energy levels including a mid-gap level. We measured capture cross sections for both electrons and holes and confirmed the mid-gap level to be a non-radiative recombination center by estimating a time constant of a non-radiative recombination. We reduced the number of the non-radiative recombination centers by high temperature growth and obtained AlGaInP with high radiative efficiency.

1. Introduction

$(\text{Al}_x \text{Ga}_{1-x})_{0.5}\text{In}_{0.5}\text{P}$ is an important material for visible laser diodes because it has a direct band gap corresponding a wavelength range from 540 ($x = 0.7$) to 680 nm ($x = 0$) and is lattice matched to GaAs¹⁾. Continuous-wave (CW) operation of these lasers with wavelengths longer than 638 nm ($x = 0.15$) has been obtained at room temperature²⁾. To make shorter wavelength lasers, x in the active layer must be increased. However, the radiative efficiency of this material tends to decrease with increasing x ³⁾. The main cause of this is non-radiative recombination centers. There have been investigations into the deep energy levels of AlGaInP^{4) 5)}. To our knowledge, however, there have been no reports examining the non-radiative recombination centers in this material.

In this paper, we present an examination of deep energy levels in undoped AlGaInP grown by metal organic vapor phase epitaxy (MOVPE) using the capacitance transient spectroscopy. We measured capture cross sections for both electrons and holes, and confirmed a non-radiative recombination

center by estimating a time constant of a non-radiative recombination, τ_{nr} .

2. Experiment

We used $(\text{Al}_x \text{Ga}_{1-x})_{0.5}\text{In}_{0.5}\text{P}$ epitaxial layers grown by low-pressure MOVPE on (100)-oriented n^+ -GaAs substrates. Al composition x ranged from 0 to 0.7. The growth temperature was varied between 670 and 730 °C with a V/III ratio of approximately 20/0. The grown layers were 2 μm thick. All samples showed n -type conductivity with a carrier concentration of 2 to $40 \times 10^{15} \text{ cm}^{-3}$, as obtained from capacitance-voltage measurements at room temperature.

We fabricated Schottky-barrier diodes and p^+n -junction diodes. We obtained the p^+n -junction by growing a p^+ -type layer doped with Zn on the undoped n -type AlGaInP layer. We made Schottky barrier contacts by Au evaporation on the epitaxial layer, and made ohmic contacts either by AuGe evaporation (n -type) or AuZn evaporation (p -type) followed by a thermal annealing at 400 °C. The diameter of the diodes ranged from 400 to 600 μm . We carried out deep level transient spectroscopy⁶⁾ (DLTS) measurements using

Schottky-barrier diodes to investigate electron traps, and we performed isothermal capacitance transient spectroscopy⁷⁾ (ICTS) measurements using p⁺ n-junction diodes to estimate the capture cross section for holes, σ_p . We measured the photoluminescence (PL) at 4.2 K and room temperature using the Ar⁺ laser 488 nm line with an excitation density of approximately 600 W/cm².

3. Results and Discussion

We measured DLTS between 80 and 500 K. We detected three electron traps (D1, D2, D3). We obtained an activation energy, E_T , and the capture cross section for electrons, σ_n , for each trap from Arrhenius plots. We calculated the concentration of each trap, N_T , from the DLTS signal intensities with subtracting the part that is not ionized in the depletion layer (the λ effect⁸⁾).

Figure 1 shows a typical Arrhenius plot. The sample was grown at 690 °C with an Al composition of 0.5. The activation energy was 0.43 eV for D1, 0.50 eV for D2, and 1.3 eV for D3. The capture cross section was 6×10^{-13} cm² for D1, 1×10^{-15} cm² for D2, and 2×10^{-10} cm² for D3. D3 has the largest σ_n .

Figure 2 plots the concentration of each trap as a function of the Al composition. Concentration decreased with decreasing x. The concentrations of D1 and D2 were both below the detection limit of 10^{12} cm⁻³ and

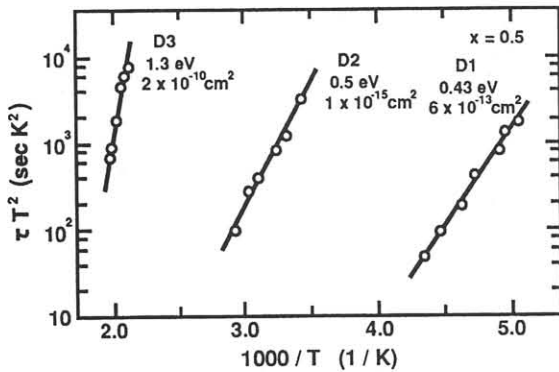


Fig.1 Arrhenius plot of the electron traps in MOVPE-grown AlGaInP ($x = 0.5$).

that of D3 was 1×10^{13} cm⁻³ at $x = 0$.

Figure 3 plots the activation energies as a function of x . The activation energies of D1 and D2 are independent of x , but that of D3 increased with x .

Figure 4 is a band diagram of AlGaInP, assuming that the conduction band offset is 40% of the band gap differences⁹⁾. D3 is located near the mid-gap and is connected to the valence band, and D1 and D2 are connected to the conduction band. This indicates that the D3 defect is composed primarily of valence-band states, and we expect D3 to interact with holes too.

We performed ICTS measurements by varying the amount of injected holes to investigate

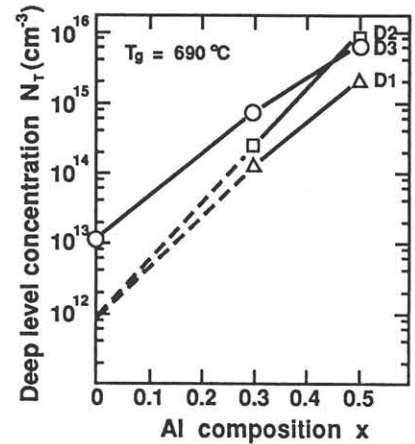


Fig.2 Concentration of the traps as a function of the Al composition. The growth temperature was 690 °C.

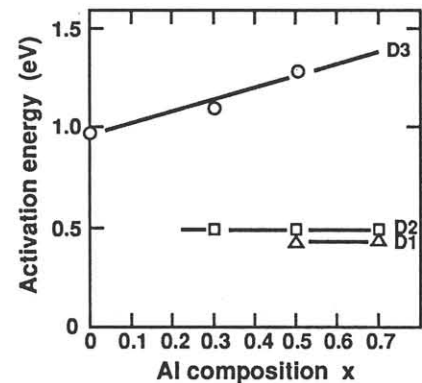


Fig.3 Activation energy of the traps as a function of Al composition.

how the electron traps interact with the valence band. When the concentration of injected holes, p , is much less than the background carrier concentration, n , the hole density captured by deep levels in pulse duration t_i is expressed as

$$p_T(t_i) = N_T [pC_p / (nC_n + pC_p)] \times \{1 - \exp[-(nC_n + pC_p)t_i]\} \quad (1)$$

$$p = (n_i^2/n) \exp(qV/kT) \quad (2)$$

where N_T is the concentration of the deep level, C_p is the capture rate for holes, C_n is the capture rate for electrons, n_i is the intrinsic carrier concentration, q is the charge, V is the forward applied voltage, k is Boltzmann constant, and T is absolute temperature. C_p and C_n are given by

$$C_p = \sigma_p v_p, \quad C_n = \sigma_n v_n \quad (3)$$

where v_p is the thermal velocity of holes and v_n is the thermal velocity of electrons. The ICTS signal intensity, S , is proportional to the captured electron density $n_T = N_T - p_T$. The following equation is obtained.

$$S(t_i)/S(\infty) - 1 = (pC_p / nC_n) \exp[-(nC_n + pC_p)t_i] \quad (4)$$

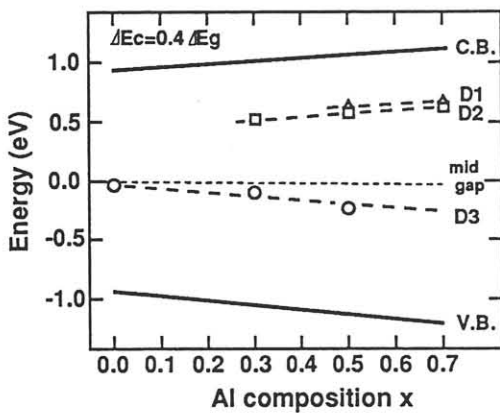


Fig.4 Band diagram of $(Al_x Ga_{1-x})_{0.5} In_{0.5} P/GaAs$. Deep energy levels are plotted using the measured activation energies.

Therefore we can calculate σ_p from the slope and the y intercept of $\log(S(t_i)/S(\infty)-1)$ and t_i .

Figure 5 plots the ICTS signal intensity of the traps as functions of the width of the hole injecting pulse, which was measured at 210 K for D1 and at 400 K for D2 and D3 with a quiescent reverse-bias voltage of -3 volts and an applied pulse height of 4.2 volts. The width of the pulse, t_i , was varied from 1 ms to 1 s. The Al composition of the sample is 0.5, and the growth temperature was 690°C. The intensity of D3 decreases as t_i increases, and saturates when t_i is 100 ms, while the intensities of D1 and D2 are independent of t_i . The sample had the carrier concentration, n , of $5 \times 10^{15} \text{ cm}^{-3}$, and p was given as approximately $2 \times 10^9 \text{ cm}^{-3}$ from equation (2). The condition described above is satisfied. We estimated σ_p of D3 to be $8 \times 10^{-16} \text{ cm}^2$ and that of D1 and D2 to be 0 using the equations (3) and (4). We see that D3 captures both electrons and holes and acts as a recombination center, but D1 and D2 are not recombination centers. We think D3 to be a non-radiative recombination center, because we detected no luminescence peak related to D3 in a PL measurement at 4.2 K. The capture cross section for holes is much less than σ_n in D3. This implies that D3 is positively ionized in thermal equilibrium.

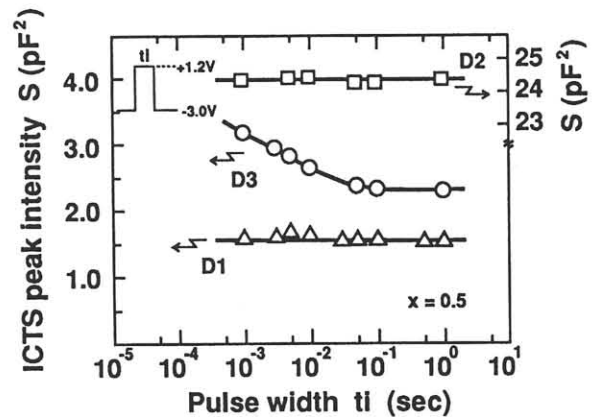


Fig.5 ICTS peak intensity of the traps as functions of the width of the hole injecting pulse. The Al composition of the sample is 0.5.

To determine whether D3 reduces the efficiency of radiative recombination, we estimated the time constant of non-radiative recombination, $\tau_{nr} = (\sigma_n v_n N_T)^{-1} + (\sigma_p v_p N_T)^{-1}$. We obtained a τ_{nr} of 15 ns. Since this value is comparable to the time constant of the radiative recombination, τ_r , calculated to from 10 ns to several hundred ns, we conclude that D3 reduces the efficiency of radiative recombination.

To increase efficiency, we need to increase τ_{nr} by reducing N_T . Figure 6 plots the PL intensity at room temperature as a function of the D3 concentration for the samples grown between 670 and 730 °C. We reduced the concentration by high temperature growth and increased the PL intensity ten times.

The D3 concentration also decreased with decreasing Al composition. We think that the source of D3 is an oxygen related defect, because aluminum reacts easily with oxygen and the incorporation of oxygen is reduced by high temperature. The lower oxygen incorporation is due to the increasing volatility of aluminum oxide¹⁰⁾.

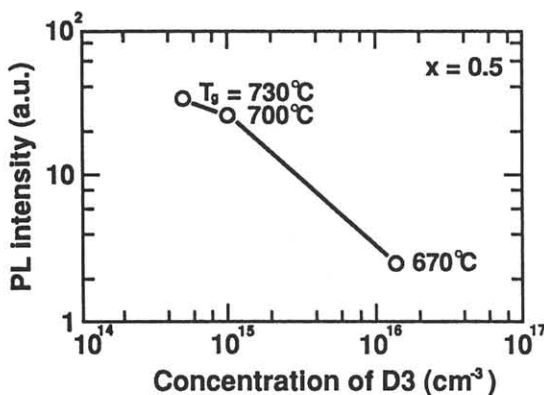


Fig.6 PL peak intensity at room temperature as a function of D3 concentration. The Al composition of the sample is 0.5.

4. Summary

We investigated deep energy levels in undoped-AlGaInP grown by MOVPE by measuring the capacitance transient spectroscopy. We detected three electron traps including a nearly mid-gap one (D3). The concentration of these traps increased with Al composition x . We concluded that D3 was a non-radiative recombination center decreasing the radiative efficiency, because it interacted with both electrons and holes, and the τ_{nr} due to D3 was comparable to τ_r . D1 and D2 did not interact with holes. We reduced the D3 concentration by high temperature growth and obtained high radiative efficiency.

References

- 1) H.Asahi, Y.Kawamura and H.Nagai ; J.Appl. Phys.53 (1982) 4928.
- 2) Y.Uematsu, G.Hatakoshi, M.Ishikawa and M. Okajima ; Proceedings of SPIE Laser-Diode Technology and Applications II, 1219(1990)2.
- 3) J.S.Yuan, C.C.Hsu, R.M. Cohen and G. B. Stringfellow ; J.Appl.Phys.57(1985) 1380.
- 4) S.Nojima, H.Tanaka and H.Asahi ; J.Appl. Phys.59 (1986) 3489.
- 5) M.O.Watanabe and Y.Ohba ; J.Appl.Phys.60 (1986) 1032.
- 6) D.V.Lang ; J.Appl.Phys.45 (1974) 3032.
- 7) H.Okushi and Y.Tokumaru ; Jpn.J.Appl.Phys. 19 (1980) L335.
- 8) Y.Zohta and M.O.Watanabe ; J.Appl.Phys. 53 (1982) 1809.
- 9) M.O.Watanabe and Y.Ohba ; Appl.Phys.Lett.50 (1987) 906.
- 10) P.D.Kirchner, J.M.Woodall, J.L.Freeout and G.D.Pettit ; Appl.Phys.Lett. 38(1981) 427.